Hybrid pore formation by directed insertion of α-haemolysin into solid-state nanopores[*]

By: Adam R. Hall, Andrew Scott, Dvir Rotem, Kunal K. Mehta, Hagan Bayley, & Cees Dekker

Made available courtesy of the Nature Publishing Group: http://www.nature.com/nnano/index.html

Abstract:
Most experiments on nanopores have concentrated on the pore-forming protein α-haemolysin (αHL)[1] and on artificial pores in solid-state membranes[2]. While biological pores offer an atomically precise structure[3] and the potential for genetic engineering[4], solid-state nanopores offer durability, size and shape control[5], and are also better suited for integration into wafer-scale devices. However, each system has significant limitations: αHL is difficult to integrate because it relies on delicate lipid bilayers for mechanical support, and the fabrication of solid-state nanopores with precise dimensions remains challenging. Here we show that these limitations may be overcome by inserting a single αHL pore into a solid-state nanopore. A double-stranded DNA attached to the protein pore is threaded into a solid-state nanopore by electrophoretic translocation. Protein insertion is observed in 30–40% of our attempts, and translocation of single-stranded DNA demonstrates that the hybrid nanopore remains functional. The hybrid structure offers a platform to create wafer-scale device arrays for genomic analysis, including sequencing[6].
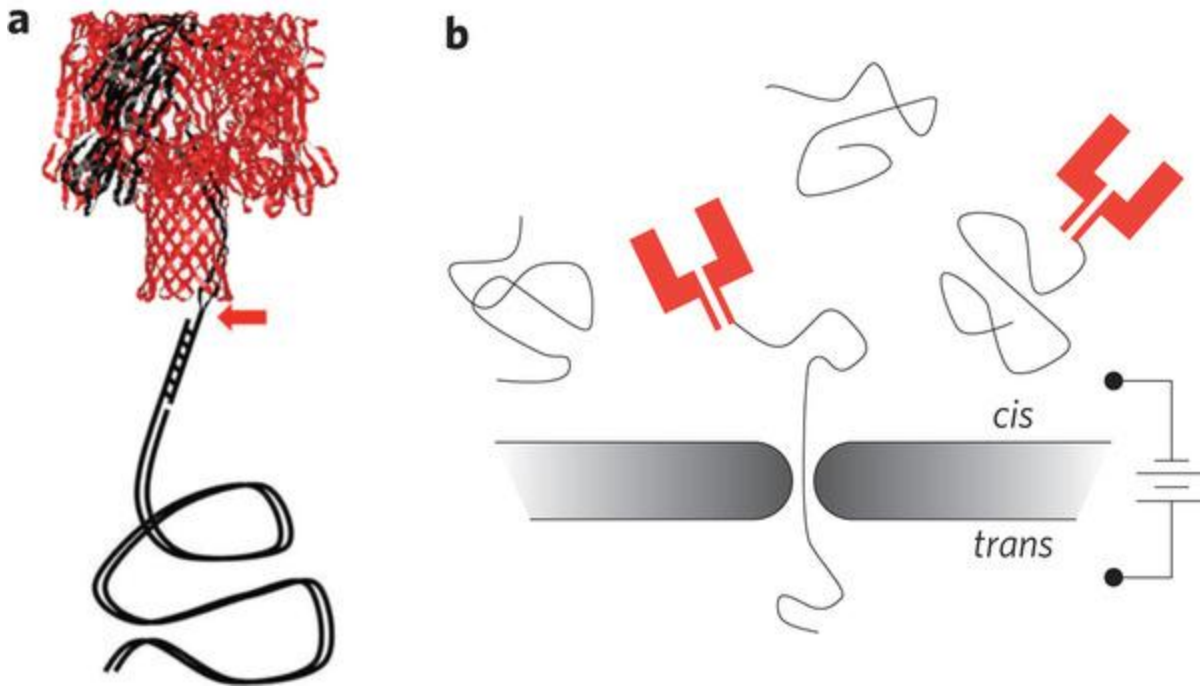Subject Terms: Nanobiotechnology, Nanomedicine

Article:
Main
We produced hybrid nanopores by inserting a single, pre-assembled α-haemolysin (αHL) protein pore into a small nanopore fabricated in a solid-state (SS) membrane. One monomer of the heptameric pore was mutated to include an additional 11-amino-acid loop at the tip of the β-barrel (**Fig. 1**a, arrow). This loop contained a single cysteine residue to which a thiol-derivatized 12-base DNA oligomer was coupled through a disulphide bond, supplying an attachment point for a long double-stranded DNA (dsDNA) molecule with a complementary single-stranded end. The result was a polyanionic tail able to guide entry of the αHL pore into the SS pore in a specific orientation. This directionality is a crucial advantage of this arrangement. Conceptually, a single αHL pore without a tethered dsDNA could also be delivered to a SS nanopore, but such protein pores would probably not end up arranged coaxially with the fabricated pores, resulting in non-functional hybrids.

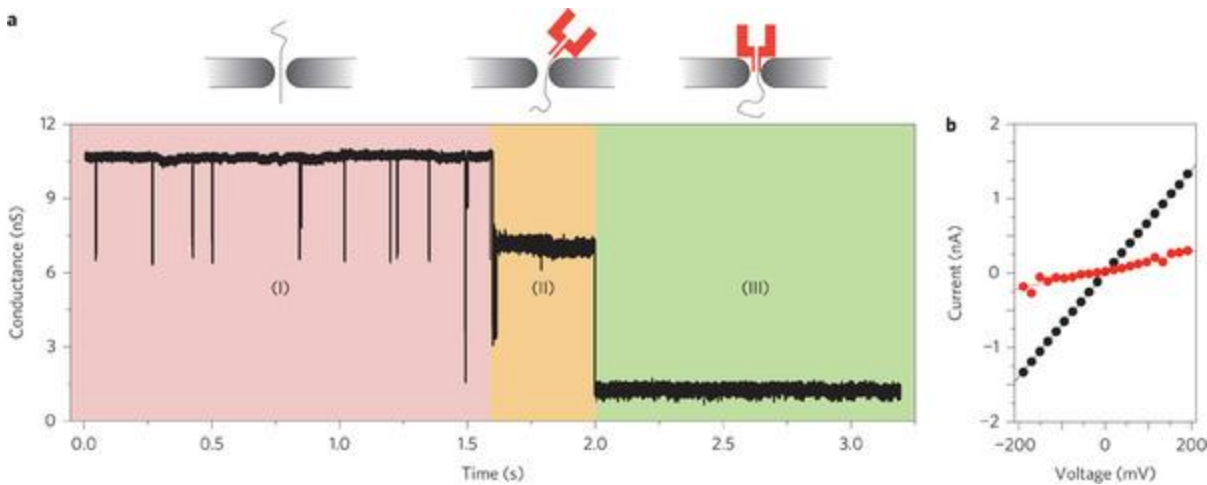**Figure 1: Molecular construct and experimental setup.**

---

a, αHL heteroheptamer with a 3 kbp dsDNA attached via a 12-nucleotide oligomer to one protein subunit. The arrow indicates the position of the disulphide at the connection point (see text). **b**, Experimental setup, in which protein-conjugated dsDNA is electrophoretically translocated through a narrow SS nanopore.

Insertion of the αHL/dsDNA construct was achieved by electrophoretic translocation (Fig. 1b). A single SS nanopore was first fabricated within a thin SiN membrane. This was used as a barrier between two reservoirs of ionic solution, with the SS pore as the only connection between the two sides. Application of an electrical potential across the membrane therefore sets up a field that is highly localized to the pore and is able to pull charged molecules through it. Importantly, these SS nanopores are fabricated with a diameter of 2.4–3.6 nm, large enough to allow the guiding dsDNA and the stem of the mushroom-shaped αHL protein pore to enter, but too small to allow the αHL cap to pass. Therefore, a dsDNA molecule will be threaded through the nanopore, pulling the attached αHL until it is stopped, mechanically, by the constriction. This will leave the cap facing the *cis* side of the membrane and the β-barrel facing the *trans* side. The small size of the SS nanopore also ensures that the dsDNA cannot be folded[7] during threading, which would lead to steric hindrance of the seal between the αHL pore and the surface of the SiN membrane.

In a typical insertion experiment, we first observe some transient changes in the measured conductance of the SS pore (Fig. 2a,I), characteristic of dsDNA translocation through a small SS nanopore[8] (Supplementary Fig. S1). These events arise from unconjugated dsDNA in the measurement solution. Such events are typically followed by a brief plateau of lower conductance (Fig. 2a,II) and then an irreversible transition to a much lower conductance level (Fig. 2a,III). We interpret the brief (<500 ms) plateau in phase II as a result of αHL-conjugated dsDNA in the pore while the protein interacts with the surrounding membrane surface and settles into position. This is supported by the fact that this plateau is always observed at about the same conductance level as the preceding dsDNA events (Supplementary Fig. S2). The final (phase III) conductance level has an average value of 1.0 ± 0.5 nS (taken over 21 observed capture events, each in a unique SS nanopore; Supplementary Fig. S3), in good agreement with the 1.0 nS conductance of αHL in lipid bilayers under the same solvent conditions[9, 10]. The variation in conductance between individual hybrid pores is probably a result of leakage currents around the αHL or slight deformation of the protein upon insertion.

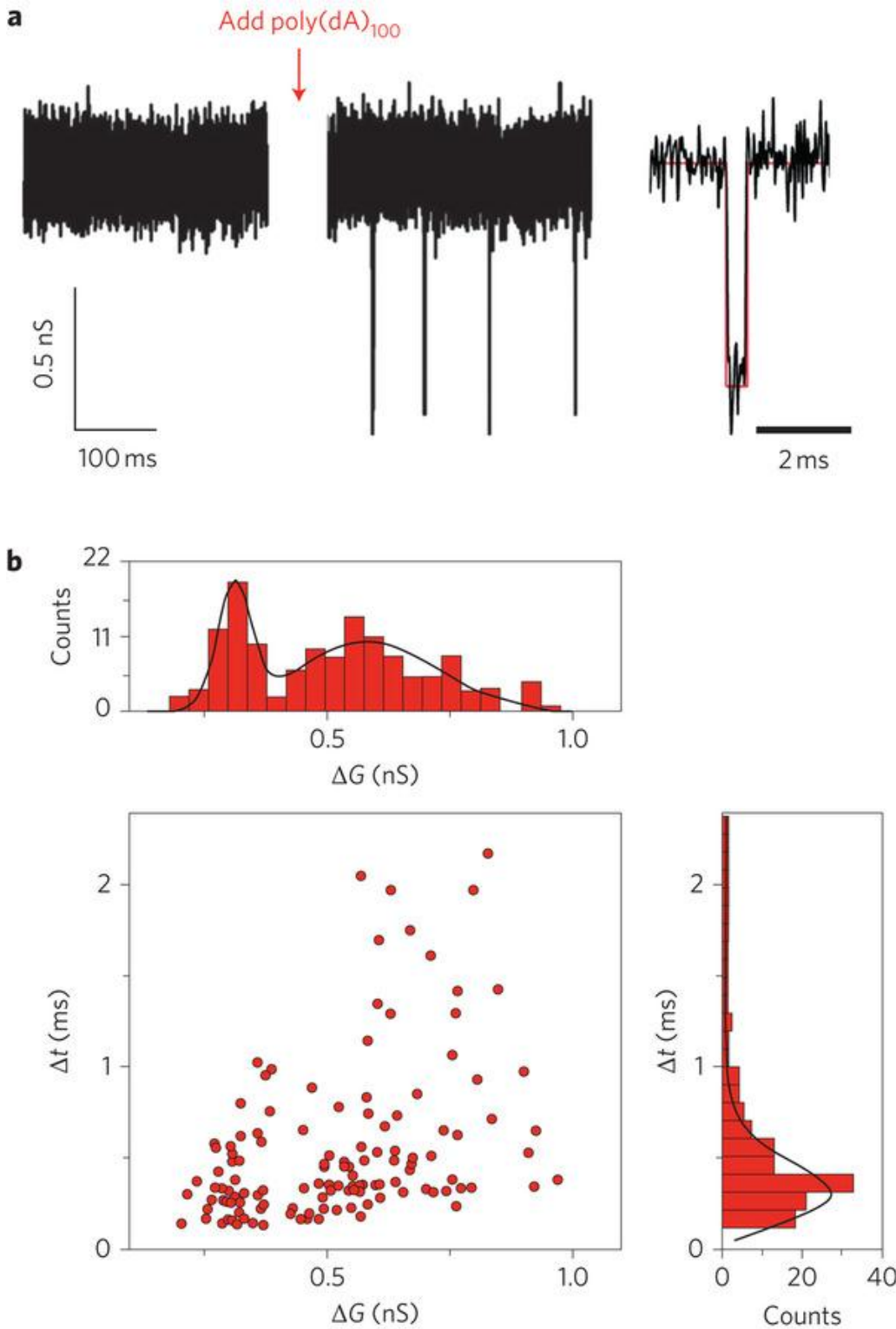**Figure 2: Directed αHL insertion.**

a, A typical event, in which an αHL protein pore inserts into a SS nanopore. The figure shows unconjugated dsDNA translocations (I), followed by a brief plateau indicating 'pre-insertion' (II), and finally a stable, low conductance level (III). A voltage of V = −600 mV was applied to the *cis* chamber. Top: sketches of the three phases in the insertion process. **b**, *I–V* response of a SS nanopore before (black) and after (red) insertion of αHL, demonstrating stability under both positive and negative applied voltages. Linear fits (solid lines) yield a resistance increase from 143 MΩ to 815 MΩ upon insertion.

Successful insertion is affected by many factors. For instance, to accommodate the protein, the initial SS nanopore must be stable within the narrow range of diameters given above. With small-diameter nanopores, changes in size and shape have been observed in solution over time due to surface rearrangement[11], which sometimes cause the SS nanopore to grow beyond the nominal size for hybrid pore production. Regardless, we observed protein insertion in 30–40% of our attempts (21 of ~60 pores). The final configuration of hybrid pores has been observed to be stable for as long as several hours, or even days (Supplementary Fig. S4). Stability could probably be improved through the use of covalent crosslinking between the protein and the SS membrane, but the hybrid structures realized in bare SS pores already demonstrate good stability under both positive and negative applied voltages (Fig. 2b).

αHL itself has a slightly positive net charge, as measured by its translocation through a 30-nm-wide SS nanopore under a positive potential (data not shown). Unconjugated proteins therefore never enter the nanopore, as they are not electrophoretically transported by the application of a negative potential to the *cis* chamber. Furthermore, the added hydrodynamic drag associated with the bulky αHL ensures that the protein approaches the pore only after the dsDNA has passed through it, in a manner that leaves the protein lodged in the constriction.

Following protein insertion, no further transient conductance changes are observed. This suggests that a single αHL pore has been inserted in the SS pore mouth, because the 1.4-nm inner diameter of the protein pore[3] is insufficiently large to allow dsDNA (diameter, 2.2 nm) to pass. Combined with the above conductance measurements, this observation is strong evidence that a single αHL pore is introduced into the SS nanopore rather than, for instance, knotted dsDNA. To demonstrate that the αHL pore is functional in the hybrid structure, we investigated the translocation of single-stranded DNA (ssDNA) as a test molecule for size selectivity. As demonstrated previously[9, 10], with a diameter of ~1.2 nm, ssDNA molecules are able to translocate through the narrow aperture of the αHL pore, and would result in translocation events if the hybrid structure were functional.

Indeed, upon the addition of single-stranded poly(dA)$_{100}$ oligomers (1 ng μl^{-1}) to the *cis* side of the chamber, transient conductance blockades are observed (Fig. 3a), indicating the passage of individual nucleic acid molecules and, importantly, demonstrating the presence of a functional, non-denatured αHL protein within the structure. Translocation events through the hybrid pore are easily resolvable with a good signal-to-noise ratio.

Figure 3: DNA translocation through a hybrid αHL/SS nanopore.

We note that Fig. 2a shows an increase in current noise following insertion of αHL, but this is not always the case (cf. Supplementary Fig. S2). Indeed, we observe that low-frequency ($1/f$) noise after αHL insertion can vary slightly compared with that of the original pore, but high-frequency noise (>1 kHz) usually remains unchanged (Supplementary Fig. S5). The latter is due to charge noise associated with the large SS membrane in contact with the measurement buffer[12], which suggests that noise levels approaching those of lipid-bound αHL could be achieved through previously demonstrated methods such as polydimethylsiloxane (PDMS) coating of the chip[13].

a, Recorded current trace through a hybrid nanopore ($V = -300$ mV, applied to the *cis* side), showing the baseline conductance directly after insertion (left) and events upon the addition of poly(dA)$_{100}$ (middle). On the right is an expanded view of a typical event (the red line indicates a square pulse fit). **b**, Event distribution of poly(dA)$_{100}$ translocations, with conductance blockade values (ΔG) and dwell times (Δt) represented as histograms above and to the right, respectively. Solid lines represent Gaussian fits to the data.

The distribution of ssDNA events recorded in a hybrid nanopore is shown in Fig. 3b (see also Supplementary Fig. S6). The measured current blockade (ΔG) of these poly(dA)$_{100}$ translocation events (Fig. 3b, top) follows a bimodal distribution, consistent with previous measurements on αHL pores in lipid bilayers[10]. Gaussian fits yield peaks centred at 0.3 and 0.6 nS, which differ somewhat from previous experiments on αHL pores in lipid bilayers, which yielded peaks at 0.8 and 0.9 nS (ref. 10). This, again, might be attributable to some leakage current around the body of the protein or deformation induced by the insertion. We find a dwell time

distribution (Fig. 3b, bottom right) with a peak value of 360 μs, in excellent agreement with the characteristic dwell time of 330 μs reported previously[10].

In summary, we have shown that individual αHL protein pores can be inserted into a SS nanopore in a controlled manner to form a functional hybrid nanopore that combines the precise structure and protein engineering possibilities associated with a biological pore with the robustness and potential required for the fabrication of an integrated device. We present three main pieces of evidence for this. First, upon insertion, the measured conductance falls to a level that agrees well with that for αHL pores in lipid bilayers. Second, at this low conductance level, there are no further signatures of translocation when only dsDNA is present in the solution. Finally, the introduction of ssDNA oligomers once again produces translocation events, demonstrating protein functionality. Without the delicate bilayer, our hybrid structures are found to be durable. For example, as a test of mechanical strength, a large voltage applied across an undrilled SS membrane yields a failure voltage of ~3 V (Supplementary Fig. S7); the highest reported voltage stability for lipid bilayers is ~800 mV in a micropipette system[14].

Importantly, incorporating the biological pore into a solid-state device opens up avenues towards the creation of wafer-scale parallel device arrays that may be useful for genomic sequencing. Future efforts towards this end will concentrate on establishing the techniques proven useful for nucleotide-specific measurements with αHL in lipid bilayers[6] into arrays of individually addressable SS nanopores. Furthermore, our measurements show that the αHL protein pore can be studied outside a lipid bilayer without lateral diffusion. In such a format, the hybrid system could be used to measure the force[15] on a single molecule within a biological pore, a physical quantity central to an understanding of the translocation process. In addition, the platform that we have established here can potentially be expanded to study different membrane proteins (transporters, receptors, and so on) through solubilization and similar attachment to a polyanionic molecule.

Materials and Methods
Solid-state nanopores
Thin (20 nm), freestanding membranes of silicon nitride were formed in silicon wafers using common microfabrication techniques[16]. The tightly focused beam of a transmission electron microscope (300 kV; beam diameter, 3.5 nm) was then used to locally ablate the membrane surface and form a single nanopore. Pore size was controlled by blanking the electron beam upon formation of a pore with the desired dimensions. Pore diameters ranged between 2.4 and 3.6 nm to ensure an optimal fit to the αHL pore. These diameters correspond to pore resistances of ~140–190 MΩ under our buffer conditions (see below). Immediately after pore formation, the membrane chip was stored in a 50% ethanol/water solution until use so as to maintain cleanliness.

Engineered αHL pores
Monomeric αHL was produced with a cysteine-containing 11-amino-acid loop (GGSSG_C_GSSGG) replacing residue 129, and an extension of 8 Asp at the C-terminus. These monomers were mixed with M113N mutant αHL monomers[4] and allowed to form heteroheptameric protein pores on rabbit red blood cell membranes. The membrane-bound proteins were then separated by sodium dodecyl sulphate polyacrylamide gel electrophoresis (SDS PAGE)[17] to obtain pores with subunits in a ratio of 1:6 ($αHL_{Cys}$:$αHL_{M113N}$), which were extracted from the gel into buffer containing 10 mM Tris-HCl, 2 mM EDTA, pH 8.5 (TE 8.5 buffer), 0.1 mM dithiothreitol (DTT) and 0.1% SDS. DTT was then removed by means of buffer replacement using centrifugal ultrafiltration (Microcon YM10). The material was stored at −80 °C between successive steps. Electrical measurements on these heteroheptamers showed that they form active pores in lipid bilayers.

In a separate process, 1 mM thiolated DNA oligomers with the sequence 5′-GGGCGGCGACCT-thiol (Sigma) in 100 μl TE buffer (pH 8.5) was treated with 10 mM DTT for 1 h at room temperature. Excess DTT was removed by five cycles of adding 200 μl ethyl acetate, vortex mixing, centrifuging at 13,000 r.p.m. for 1 min, and removal of the organic phase. The oligomers were passed over a Bio-Spin P6 column (BioRad) pretreated with TE 8.5 buffer and then incubated with 10 mM 2,2′-dipyridyl disulphide (Aldrich) for 1.5 h at room

temperature. Excess dipyridyl disulphide was removed by five cycles of adding 200 μl diethyl ether, vortex mixing, centrifuging at 13,000 r.p.m. for 1 min, and removal of the organic phase. Activated oligomers were added to the purified heteroheptamers, followed by a centrifugal ultrafiltration (Microcon YM50) to remove excess DNA. The material was stored at −80 °C before use.

Protein–DNA construct

λ-phage DNA (New England Biolabs) was digested with the restriction enzyme SfoI. This enzyme leaves blunt ends, resulting in two fragments (45679 bp cosL and 2823 bp cosR), each with a 12-nt overhang. Gel purification was performed to select the smaller fragment (overhang sequence 5′-AGGTCGCCGCCC), which was subsequently hybridized with the complementary oligomer attached to the heteroheptamer described above by incubation for 30 min at room temperature.

Ion current measurements

A chip with a single solid-state nanopore was mounted in a custom flow cell, and measurement solution (1 M KCl, 10 mM Tris buffer, pH 8.0) was added to both sides of the membrane. Electrical measurements were performed using Ag/AgCl electrodes attached to a patch-clamp amplifier (Axopatch 200B, Axon Instruments). Signals were acquired at 200 kHz and low-pass-filtered at 20 kHz before digitization. For the poly(dA)$_{100}$ translocation experiments in Fig. 3 and Supplementary Fig. S6, the conductance blockade (ΔG) of each event was defined as the difference between the average baseline and the average event level ($G_0 - G_{event}$).

References

Branton, D. et al. The potential and challenges of nanopore sequencing. Nature Biotechnol. 26, 1146–1153 (2008).

Dekker, C. Solid-state nanopores. Nature Nanotech. 2, 209–215 (2007).

Song, L. Z. et al. Structure of staphylococcal alpha-hemolysin, a heptameric transmembrane pore. Science 274, 1859–1866 (1996).

Bayley, H. & Jayasinghe, L. Functional engineered channels and pores. Mol. Membr. Biol. 21, 209–220 (2004).

Storm, A. J. et al. Fabrication of solid-state nanopores with single-nanometre precon. Nature Mater. 2, 537–540 (2003).

Clarke, J. et al. Continuous base identification for single-molecule nanopore DNA sequencing. Nature Nanotech. 4, 265–270 (2009).

Storm, A. J. et al. Fast DNA translocation through a solid-state nanopore. Nano Lett. 5, 1193–1197 (2005).

Wanunu, M. et al. DNA translocation governed by interactions with solid-state nanopores. Biophys. J. 95, 4716–4725 (2008)

Akeson, M. et al. Microsecond time-scale discrimination among polycytidylic acid, polyadenylic acid, and polyuridylic acid as homopolymers or as segments within single RNA molecules. Biophys. J. 77, 3227–3233 (1999).

Meller, A. et al. Rapid nanopore discrimination between single polynucleotide molecules. Proc. Natl Acad. Sci. USA 97, 1079–1084 (2000).

van den Hout, M. et al. Controlling nanopore size, shape and stability. Nanotechnology 21, 115304 (2010).

Smeets, R. M. M. et al. Noise in solid-state nanopores. Proc. Natl Acad. Sci. USA 105, 417–421 (2008).

Tabard-Cossa, V. et al. Noise analysis and reduction in solid-state nanopores. Nanotechnology 18, 305505 (2007).

White, R. J. et al. Single ion-channel recordings using glass nanopore membranes. J. Am. Chem. Soc. 129, 11766–11775 (2007).

Keyser, U. K. et al. Direct force measurements on DNA in a solid-state nanopore. Nature Phys. 2, 473–477 (2006).

Krapf, D. et al. Fabrication and characterization of nanopore-based electrodes with radii down to 2 nm. Nano Lett. 6, 105–109 (2006).

Howorka, S., Cheley, S. & Bayley, H. Sequence-specific detection of individual DNA strands using engineered nanopores. Nature Biotechnol. 19, 636–639 (2001).